X-ray scattering measurements of Fused Silica samples after Ion Beam Figuring

Issued by ***B. Salmaso*** and ***D. Spiga*** (INAF/OAB)

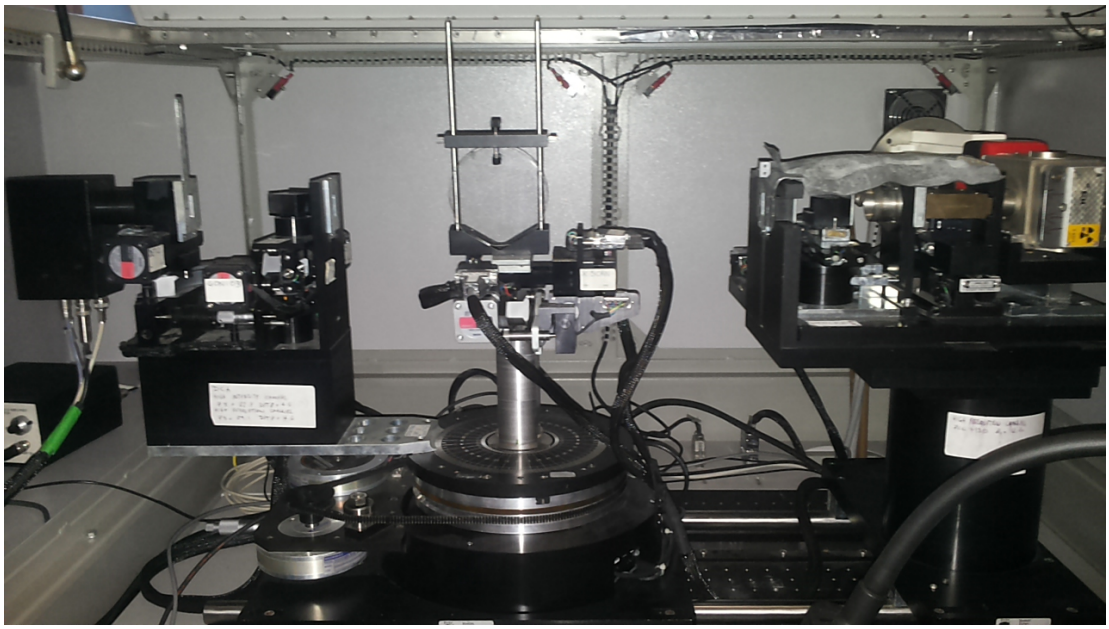

Fig. 1: The BEDE-D1 diffractometer at INAF-OAB and the setup for X-ray scattering measurements on the Fused Silica samples

Istituto Nazionale di Astrofisica (INAF)

Via del Parco Mellini, 00100 Roma, Italy

Osservatorio Astronomico di Brera (OAB)

Via Brera 28, 20121 Milano, Italy

Via E. Bianchi 46, 23807 Merate, Italy

Contents

Reference Documents

[RD1]. Civitani M., Citterio, O., Gigo, M., Mattaini, E., Prareschi, G., Parodi, G., *Thin monolithic glass shells for future high angular resolution and large collecting area x-ray telescope*, Proc. SPIE 8884, 88841R (2013)

[RD2]. Pareschi, G., Basso, S., Civitani, M., Ghigo, M., Parodi, G., Pelliciari, C., Salmaso, B., Spiga, D., Vecchi, G., *Beyond Chandra (towards the X-ray Surveyor mission): possible solutions for the implementation of very high angular resolution X-ray telescopes in the new millennium based on fused silica segments*, Proc. SPIE 9905, 99051T (2016)

[RD3]. Holyszko, J., Salmaso, B., Ghigo, M., *Roughness degradation of fused silica samples after Ion Beam Figuring*, INAF/OAB internal report 05/2017

[RD4]. Windt, D.L., *IMD-software for modeling the optical properties of multilayer films*, Computers in physics, Vol. 12, no.4 (1998)

[RD5]. Church, E. L., Takács, P. Z., *Interpretation of glancing incidence scattering measurements*, Proc. SPIE 640, 126 (1986)

[RD6]. Spiga, D., Raimondi, L., Salmaso, B., et al., *High-resolution X-ray scattering measurement of slumped glasses*, INAF/OAB internal report 04/2011

Acronyms

IBF	Ion Beam Figuring
MFT	Micro Finish Topographer
PSD	Power Spectral Density
FS	Fused Silica
WFXT	Wide Field X-ray Telescope
XRR	X-ray Reflectivity
XRS	X-ray Scattering

1 Introduction

A Fused Silica segment (segment#4), obtained by cutting the broken WFXT shell #7 [RD1], was processed in 2016 with the Ion Beam Figuring (IBF) facility present at INAF-OAB, in order to impart the correct Wolter I shape [RD2]. The sample was positioned at 36 mm distance from the source, a standard distance for all the processes performed at INAF/OAB. After this process, the optical surface was found covered by peaks (Fig. 2-left) of material that was determined to be Fused Silica (FS) by SEM micro-analysis [RD3]. The roughness of this sample increased from 1 nm before IBF to 2.2 nm after IBF. To mitigate the problem, two additional Fused Silica flat samples were processed with IBF at 36 and 76 mm distance, and their roughness was measured with the Micro Finish Topographer (MFT) also present in OAB laboratories. The Power Spectral Density (PSD) of these two samples, obtained from roughness measurements with the 10× magnification objective, was compared with the PSD obtained from a brand new Fused Silica sample, proving a 70 mm distance as appropriate to minimize the problem (Fig. 2-right).

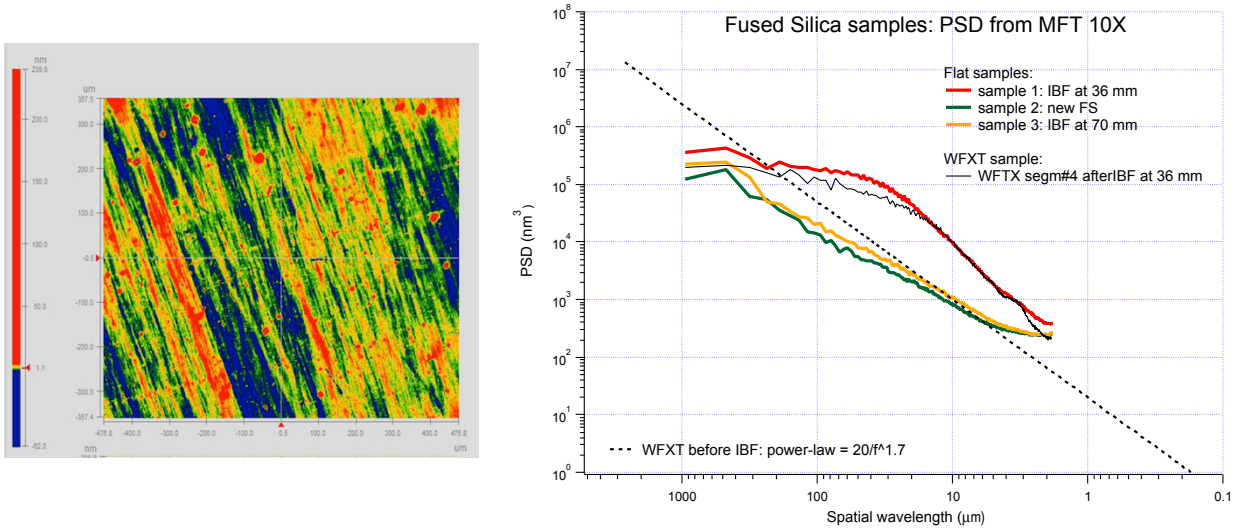

Fig. 2: Left: MFT 10× image taken on the segment#4 cut from the broken WFXT shell#7, after IBF performed at 36 mm distance from the source (rms = 2.2 nm). The roughness of this sample, before IBF, was 1 nm rms on the same spatial wavelength range. Right: the PSD from roughness measurements taken with the MFT 10×. The PSD of the segment#4, processed with IBF at 36 mm distance from the source, (black line) matches the PSD of the flat sample#1, also processed at 36 mm distance (red line). The PSD of the sample#3, processed at 70 mm distance, almost matches the PSD of the brand-new sample#2. The dotted black line corresponds to the power law that best fits the roughness of the WFXT segments before the IBF process.

In this report, we present the results of the X-ray Scattering (XRS) measurements performed on the three FS flat samples, with the BEDE-D1 diffractometer operated at OAB. The aim is to confirm that the peaks appearing on the sample surfaces after IBF at 70 mm distance contribute to scatter X-rays, in addition to the scattering off the background topography. This is a useful step to confirm that the complete roughness PSD, including the contribution of peaks, actually contributes to the X-ray scattering degrading the image. Shortly put, these measurements will tell us to which extent we should be concerned by these peaks in the surface topography.

2 X-Ray Scattering modelling

2.1 Theoretical background

The X-ray scattering off a reflective surface, at a light wavelength λ, can be computed by using the first order perturbation theory in grazing incidence, assuming the surface to be smooth and isotropic. We consider X-rays (Fig. 3), of wavelength λ, impinging on a surface at a grazing incidence angle θ_i, and scattered off the surface with a scattering angle θ_s.

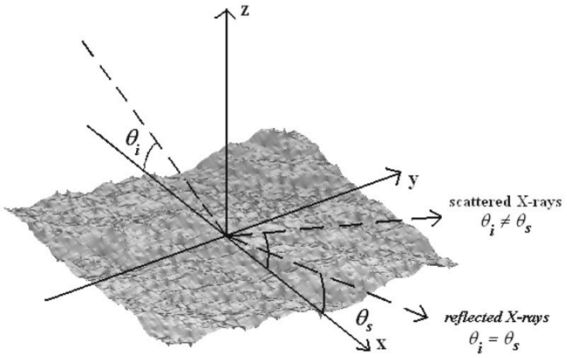

Fig. 3: Sketch of an incident ray incident on a rough surface: θ_i is the incidence angle and θ_s is the scattering angle.

For a single boundary characterized by a single PSD, the relation is a simple proportionality between the scattered intensity per angle unit and the mono-dimensional PSD, $P(\nu)$, where ν is the spatial frequency of the Fourier components of the rough profile in the incidence plane [RD5]:

$$\frac{1}{I_0}\frac{dI_s}{d\theta_s} = \frac{16\pi^2}{\lambda^3} Q_{is} \sin^2\theta_s \sin\theta_i P(\nu) \qquad \text{(Eq. 1)}$$

The spatial frequencies ν are related to the X-ray wavelength, the incident angle and the scattering angle by:

$$\frac{1}{\nu} = \frac{\lambda}{|\cos\theta_s - \cos\theta_i|} \qquad \text{(Eq. 2)}$$

The polarization factor $Q_{is} = \sqrt{R(\theta_s)R(\theta_i)}$ in the Rayleigh-Rice vector theory is obtained from the reflectivity values R computed via the generalized Fresnel equations.

2.2 Implementation in the IDL code

The implementation of Eq. 1 in a code is done knowing that:

1) dI_s is obtained from a direct photon rate count when the sample is irradiated at the incidence angle θ_i and the detector scans the reflected /scattered beam at various angles within an angular range $d\theta_s$;
2) $d\theta_s$ is given by the FWHM of the direct beam scan with the detector mounting the same collimating slit used to scan the scattered beam. This scan also allows us to understand where the scattered beam falls below the background level;

3) the normalization factor I_0 is obtained from the integration of the measured scattering scan; this is a better choice than deriving it from the direct beam, since the count rate typically decreased during the direct beam scan (lasting 3 hours). The scattering measurement is acquired when the count rate has become stable;
4) Q_{is} is computed from the reflectivity ratio $\sqrt{R(\theta_s)/R(\theta_i)}$, because the normalization is done with the scattered beam, rather than the direct beam;
5) the Fresnel reflectivity values are computed at the measured scattered angles, using an hoc written IDL code, because the reflectivity computed with IMD [RD4] can only be sampled at regular angular steps.

2.3 Tuning the incidence angle at 8.045 keV

The BEDE-D1 diffractometer is used in the monochromatic mode of 8.045 keV (Cu-Kα line). We are really interested in the assessment of scattering at 1 keV, so at 8.045 keV we have to use an incidence angle smaller than the nominal one (0.71 deg, for the Wolter that best fit the segment shape: diam = 486 mm, focal = 4900 mm) in order to keep the ratio $\lambda/\sin\theta_i$ at the same value (100 nm). In fact, it is easily seen that, for $\theta_s \approx \theta_i$, Eq. 1 does not depend on incidence angle and the X-ray wavelength, but only on the ratio $\lambda/\sin\theta_i$, and so do the expression of the reflectivities and - in the limit $\theta_s \approx \theta_i$ - also Eq. 2. Therefore, it is fair to say that the scattering measurement at 8.045 keV (1.541 Å) is representative of the scattering level expected on the mirror shell, provided that the ratio $\lambda/\sin\theta_i$ is conserved. This entails an appropriate value for the incidence angle at arcsin(1.541 Å / 100 nm) = 318 arcsec.

3 XRS setup and measured samples

The BEDE-D1 diffractometer was used to measure the XRS from the FS samples. A Pb shield (Fig. 1) was positioned over the monocromation stage after the X-ray source, in order to reduce the measured background and enable the XRS measurements at large scattering angles, where the signal is - typically - less intense. A slit of 50 µm was positioned at the exit of the monochromation stage, while a slit of 400 µm was positioned in front of the detector. The FWHM of the direct beam, measured with this setup, was 300 arcsec.

The scattering measurements were taken from the 0 deg scattering angle (i.e. aligned with the sample surface) up to 2 deg off-surface. The angular steps were of 7.2 arcsec and the integration time for each step was of 10 sec, which entailed a measuring time of about 3 hours per single scan.

The sample surface covered by the beam - and therefore generating scattering - was about 20 mm in height (determined by the source slit height) and 100 mm in length (the full sample length).

The FS samples were positioned on a support fixed to the goniometer by a screw. Three FS samples were measured (see [RD3] for more detailed description on the IBF parameters used):

- sample 1: processed with IBF at 36 mm distance from the source, to remove a constant thickness;
- sample 2: the back side of a sample processed with the Zeeko present in OAB, considered as a brand new, unprocessed, reference surface;
- sample 3: processed with IBF at 70 mm distance from the source, still to remove a constant thickness but at a “safer” distance than sample 1.

4 XRS measurements

XRS measurements were taken on the three samples, and were compared with the direct beam scan. Fig. 4 shows the scattering decreasing, going from sample 1 to sample 3, processed at 36 and 70 mm distance respectively. This is qualitatively in agreement with the decreasing roughness PSD measured with the MFT, as shown in Fig. 2. The sample 2 (green line, the reference sample) also produces some scattering: the surface is smoother but still exhibits surface imperfections that bring the surface rms to 8.5 Å.

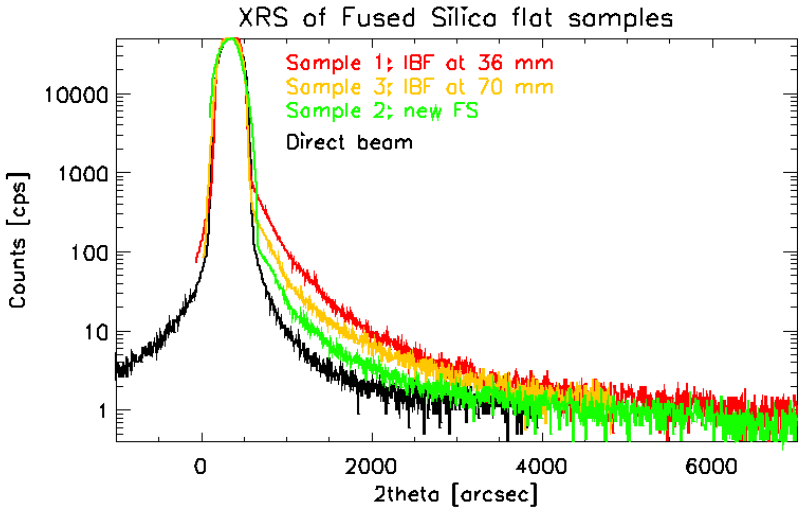

Fig. 4: XRS scans at 8.045 keV and 315 arcsec of the Fused Silica samples, compared with the direct beam (black line). The red line is sample 1, processed with the IBF source at 36 mm distance. The orange line was obtained from sample 3, processed with the IBF source at 70 mm distance. Green line represents the sample 2, the only unprocessed sample.

5 PSD computed from XRS scans and MFT 10×

Using Eq. 1 and Eq. 2, the PSD of the surface contributing to scattering was computed from the XRS of the three samples that lies above the direct beam. The results are shown in Fig. 5.

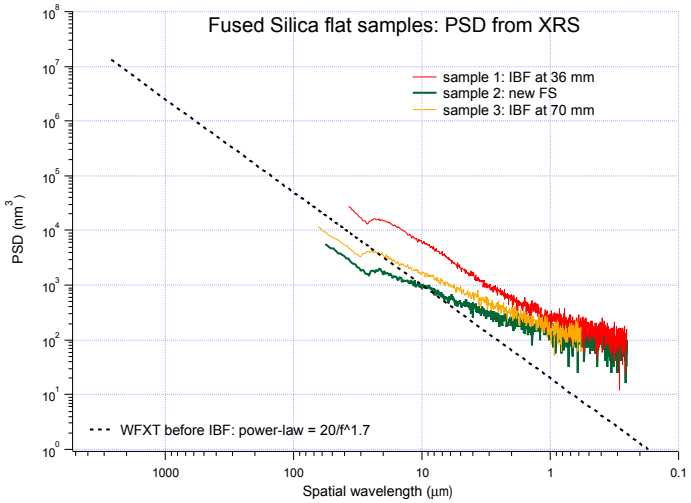

Fig. 5: PSD computed from XRS measurements at 315 arcsec incidence angle, for the three samples. The dotted black line corresponds to the power law that fits the roughness of the WFXT segments before the IBF.

The PSD computed from XRS was overplotted to the PSD computed from roughness data obtained with the MFT 10×. Samples #2 and #3 showed a good agreement between the PSD from XRS and from MFT. In contrast, sample#1 had initially the two PSDs mismatching each other, because only 3 measurement locations had been measured with the MFT. The sample is, however, markedly inhomogeneous (rms values: 2.78-3.47-2.29 nm, see Table 1) and so the peak distribution could have not been sampled correctly. In contrast, the PSD obtained measuring the XRS scan is highly representative of the surface sample because several cm^2 were sampled vs. the few mm^2 typically covered by an MFT image.

Meas	rms [nm]
1	2.78
2	3.47
3	2.29
4	1.46
5	4.47
6	3.37
7	1.45
8	1.65
9	1.51
10	1.73

Table 1. The rms obtained on 10 different positions of sample#1 with the MFT 10×.

We have therefore improved the sampling of the surface roughness with the MFT on sample #1, taking the number of measurements to 10. Measurements visibly contaminated by dust or major surface defects were removed from the PSD averaging (positions 2-5-6 of Table 1). The results of the PSD comparison are presented in Fig. 6 for sample#1, and Fig. 7-8 for samples #3-2.

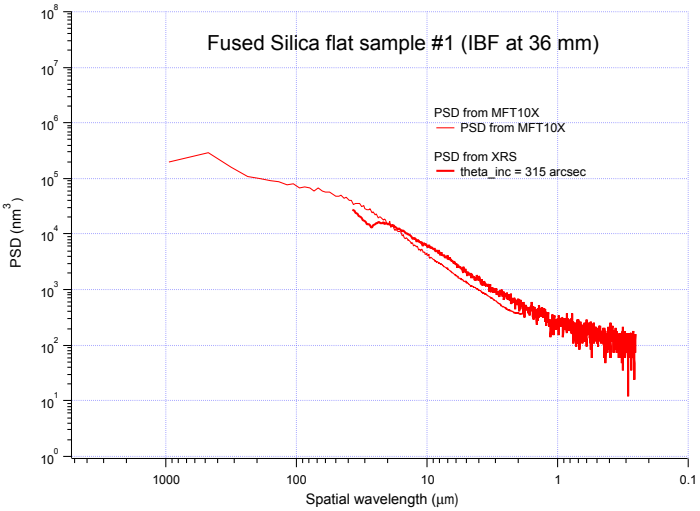

Fig. 6: Sample #1: matching of the PSD computed from an XRS measurement at 315 arcsec incidence angle and the PSD computed from the roughness data obtained with the MFT 10×.

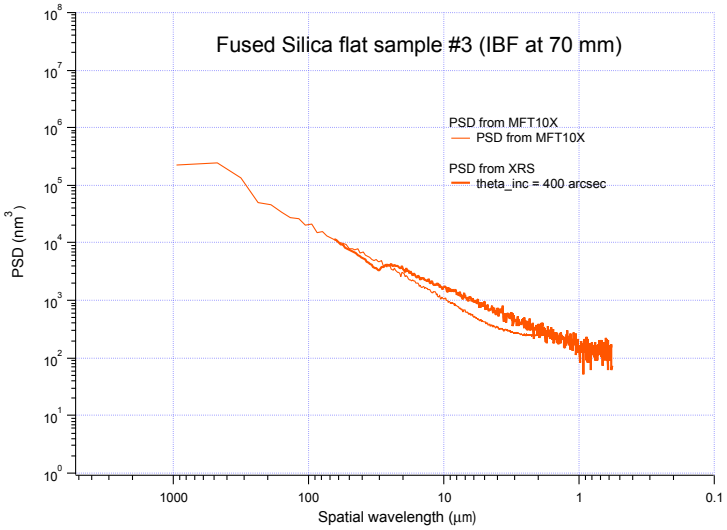

Fig. 7: Sample #3: matching of the PSD computed from an XRS measurement at 315 arcsec incidence angle and the PSD computed from the roughness data obtained with the MFT 10×.

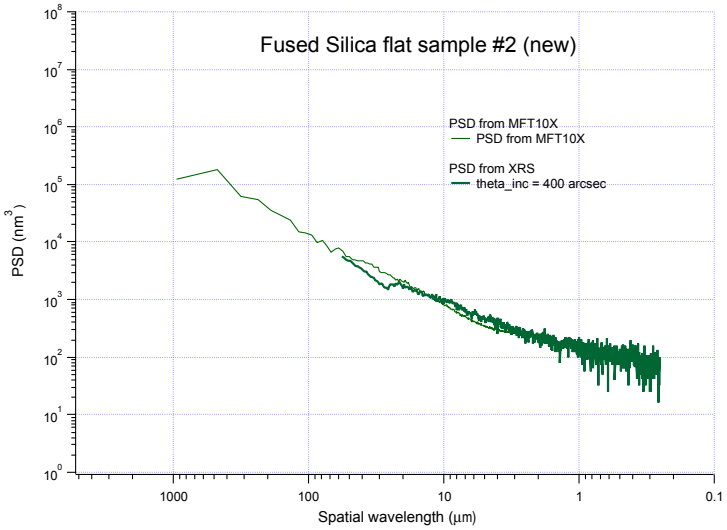

Fig. 8: Sample #2: matching of the PSD computed from an XRS measurement at 315 arcsec incidence angle and the PSD computed from the roughness data obtained with the MFT 10×.

6 Impact of peaks on the PSD shape

To the aim of disentangling the effects on the PSD of the peaks introduced by the IBF on the Fused Silica samples working at 36 mm distance from the source, from the effects introduced by the polishing defects (shown as lines defects in Fig. 2-left), one of the image obtained from the MFT 10× on the WFXT segment#4 after the IBF process (Fig. 2-left), was mathematically filtered to remove the peaks. The heights were binned in order to consider only the heights below the 95 or the 90 percentile. The resulting images are presented in Fig. 9, showing that the peaks were mathematically removed, but keeping the scratches unchanged. The PSDs computed from those images are presented in Fig. 10, showing that the hump in the red PSD disappears when the peaks are removed and it is therefore closely related to the peaks themselves.

All data	Below 95 percentile	Below 90 percentile
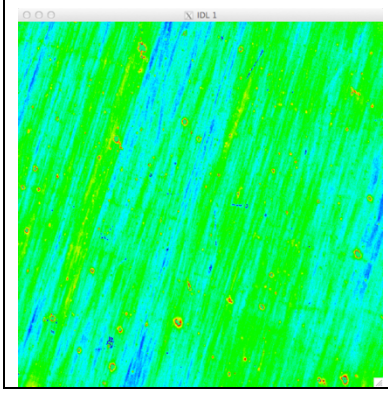	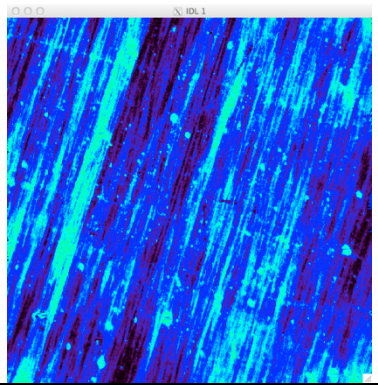	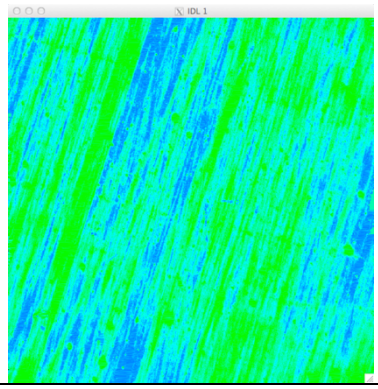

Fig. 9: Peak filtering in the image in Fig. 2-left. The peaks were progressively removed using a z-filter; already removing height data beyond the 90th percentile the peaks disappear completely.

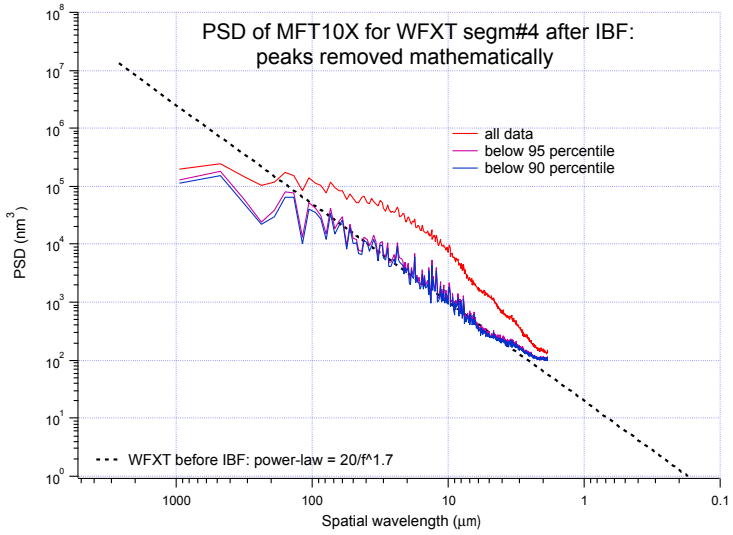

Fig. 10: the PSDs obtained by removing the peaks in Fig. 2-left with the procedure described in this paragraph. The peaks are responsible for a noticeable PSD increase and cannot be ignored. Moreover, the agreement between the PSD obtained from XRS and the PSD hump shows that the peaks actually play a relevant role in the X-ray scattering.

7 Conclusions

This work reports the X-Ray scattering measurements performed with the BEDE-D1 equipment on Fused Silica flat samples. Two samples (sample#1 and #3) were previously processed with the IBF at different distances from the source, in order to minimize the defects (also made of Fused Silica, as proven by SEM micro-analysis) introduced by the process itself on the optical surface. One sample (#2) was kept unprocessed and served as reference. The sample #1, processed at the closest distance (36 mm from the IBF source), was processed with the same parameter of the curved WFXT segment#4, figured at the IBF to the aim of correcting the segment shape to the desired Wolter parameters.

The samples were found to produce scattering to an extent dependent on their roughness, as measured with the MFT 10×, and the XRS level turned out to be in agreement with the PSD computed from the complete MFT maps, including the peaks. In particular, the sample#1, the one with the highest roughness and with the highest density of peak defects in the topographic maps, returned the highest scattering level and the PSD computed from the XRS diagrams was in agreement with MFT measurements. Since the peaks represent the dominant term of the PSD degradation and the PSD would have been completely different if no peak were present, we conclude that ***the peaks present on the surfaces DO contribute to the X-ray scattering, as per the 1st order scattering theory***.

Moving the sample from 36 to a 70 mm distance does reduce the roughness and therefore the scattering, again in agreement with the 1st order theory (Eqs. 1 and 2). This shows which pathway should be followed in the development of the IBF process for thin shells.